Separation and Purification Technology 363 (2025) 132139

Contents lists available at ScienceDirect

Separation and Purification Technology

journal homepage: www.elsevier.com/locate/seppur

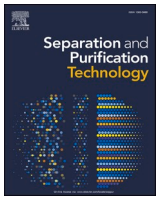

Removal of polystyrene nanoplastics from urban treated wastewater by electrochemical oxidation☆

Alejandro Pérez-López, Carmen M. Domínguez, Aurora Santos, Salvador Cotillas *

Department of Chemical Engineering and Materials, Faculty of Chemical Sciences, Complutense University of Madrid, Avenida Complutense s/n, 28040 Madrid, Spain

ARTICLE INFO

Editor: Dr. B. Van der Bruggen

Keywords:
Nanoplastics
Toxicity
Electrochemical oxidation
Boron doped diamond anode
Mixed metal oxide

ABSTRACT

This work investigates for the first time the removal of polystyrene nanoplastics (NPs) from synthetic urban treated wastewater by electrochemical oxidation with Boron-Doped Diamond (BDD). The influence of current density (10–100 mA cm^{-2}) and initial pollutant concentration (20–100 mg L^{-1}) was evaluated. Additionally, the effect of the anode material on NPs removal was studied, employing Mixed Metal Oxide (MMO) anodes. The process efficiency was assessed through Total Organic Carbon (TOC) reduction and acute toxicity tests using the *Aliivibrio fischeri* luminescent bacterium. Results demonstrate that BDD anodes achieve mineralisation rates exceeding 90 % at current densities above 50 mA cm^{-2}, whereas MMO anodes exhibit significantly lower degradation. Due to competing reactions, such as oxygen evolution, the process efficiency decreases at higher current densities with BDD anodes. NPs removal occurs primarily by a mediated oxidation process involving electrochemically generated oxidants. After treatment, transmission electron microscopy (TEM) analysis reveals a progressive reduction in NPs size from 150 nm to 68 nm. Regarding toxicity analysis, acute toxicity can be eliminated by applying current densities above 50 mA cm^{-2}, indicating that the generated by-products are non-toxic. These findings highlight the feasibility of electrochemical oxidation with BDD anodes for removing NPs from urban treated wastewater since the experimental conditions used in the previous literature often differ significantly from those in real wastewater. The study underscores its potential as a sustainable technology to mitigate the spread of these emerging pollutants into the environment.

1. Introduction

Plastics are versatile raw materials used to produce countless products for different applications. In 2022, the global production volume of plastics exceeded 350 million tons due to their excellent physical–chemical properties and low cost [1]. However, the main drawbacks of these polymers are their lifetime (single use in many cases) and the challenges associated with the management of plastic wastes, which accumulate in landfills and natural ecosystems (including the aquatic environment) [2]. Currently, only 8.9 % of plastics production comes from mechanically or chemically recycled post-consumer materials, while more than 90 % is derived from fossil-based sources [3]. As a result, plastic wastes persist in the environment, undergoing physical and chemical degradation processes that can produce secondary microplastics (MPs) and nanoplastics (NPs) [4,5]. MPs include plastic particles between 1 μm and 5 mm in size, whereas particles smaller than 1 μm are considered NPs. Under this growing concern, micro(nano) plastics (MNPs) pollution was recognised in 2016 as the second most important scientific issue in environmental sciences research by the United Nations Environment Assembly [6].

On the other hand, primary MNPs are plastics intentionally manufactured at the micro and nanoscale for specific applications. They can also be found in the environment, although the amount of NPs is lower than that of MPs [7,8]. Traditionally, research has predominantly focused on the hazardous properties and the environmental impact of MPs [4,9,10]. Nonetheless, the number of publications that explore the characteristics and potential risks of NPs in the environment has increased considerably [11–14].

Despite the acceptance that MNPs end up in the oceans [15], recent studies demonstrate that the concentration of MNPs in freshwater may be similar or even higher than in the marine environment [6,16,17]. One of the primary sources of this type of pollution is urban Wastewater Treatment Plants (WWTPs) [17–19]. Although these facilities can remove 90 % of MNPs [6,20], mainly retained in the sludge, the large

☆ This article is part of a special issue entitled: 'Sustain energy & environ' published in Separation and Purification Technology.

* Corresponding author.
E-mail address: salvacot@ucm.es (S. Cotillas).

https://doi.org/10.1016/j.seppur.2025.132139
Received 30 November 2024; Received in revised form 14 February 2025; Accepted 17 February 2025
Available online 18 February 2025

volumes of wastewater processed imply that the treated effluents still contain significant amounts of the smaller fractions, i.e., NPs [21]. This is because the existing physical–chemical and biological technologies in urban WWTPs cannot remove NPs from wastewater, and hence, they can be considered emerging pollutants. For this reason, it is necessary to develop clean and sustainable technologies capable of removing NPs from urban treated wastewater to avoid the dispersion of these pollutants in the environment.

In this context, recent studies have positioned electrochemical oxidation (EO) as a promising alternative for degrading recalcitrant organic pollutants from aqueous phases [22,23]. This technology is based on generating powerful oxidants and free radicals from the oxidation of the ions naturally contained in the effluents and water oxidation [24]. These oxidants and radicals attack the pollutants until their complete degradation or total mineralisation [25].

Kiendrebeogo et al. [26] have reported the electrochemical degradation of NPs in sulphate media (1000 mg L^{-1} Na_2SO_4) using a boron-doped diamond (BDD) anode and titanium (Ti) and carbon felt (CF) as cathodes. The study achieved a 90 % removal of 10 mg L^{-1} polystyrene nanospheres after 6 h of treatment using the CF cathode to promote H_2O_2 production under acidic conditions at a current density of 36 mA cm^{-2}. However, the removal percentage decreased below 80 % when Ti was used as a cathode under the same operating conditions, obtaining a mineralization percentage of 56.2 %. Other studies have investigated the application of other Advanced Oxidation Processes (AOPs) for the degradation of NPs in ultrapure water. Di Luca et al. reported the complete mineralisation of 20 mg L^{-1} polystyrene nanoplastics within 40 min by photo-Fenton process [27]. Similarly, Nabi et al. employed photodegradation using TiO_2 nanoparticles under ultraviolet light irradiation, achieving the total NPs mineralisation after 12 h [28]. Previous studies have demonstrated the ability of AOPs (including electrochemical technologies) to remove NPs in water. However, the experimental conditions studied in these works often differ significantly from those in real wastewater scenarios. Therefore, the conclusions drawn should be validated using real effluents or complex solutions that closely simulate real compositions. To the authors' knowledge, treating urban treated wastewater polluted with NPs has not yet been conducted. The physical–chemical composition of these complex effluents can significantly influence the NPs degradation.

With this background, this work focuses on studying the removal of polystyrene NPs in urban treated wastewater by electrochemical oxidation. BDD and Mixed Metal Oxide (MMO) electrodes were used as the anode, and stainless steel (SS) was used as the cathode. The influence of the current density (j: 10—100 mA cm^{-2}) and the initial pollutant concentration ([NPs]: 20 – 100 mg L^{-1}) on NPs removal was evaluated. The acute toxicity of the treated effluents was evaluated using the *Aliivibrio fischeri* luminescent bacterium. The results obtained in this work open the door to applying the technology studied to treat complex effluents polluted with NPs, such as the tertiary treatment in WWTPs.

2. Materials and methods

2.1. Chemicals

Monodisperse polystyrene nanospheres PS-R-KM248 ($D_0 = 150 \pm 5$ nm 5 % w/v) were purchased from microParticles GmbH. Synthetic urban treated wastewater was prepared based on the analytical grade of magnesium sulphate, sodium acetate (Fisher Scientific), sodium chloride (Acros), ammonium chloride, potassium sulphate, sodium sulphate (Panreac), sodium phosphate and sodium nitrate (Sigma Aldrich). Sulfuric acid (Fluka), potassium iodide (Fisher Scientific) and starch solution (Panreac) were employed to determine the concentration of total oxidants. Sodium carbonate (Panreac), sodium bicarbonate, nitric acid, oxalic acid (Sigma Aldrich), sulfuric acid (Fluka) and acetone (VWR) were used as the mobile phases for ion chromatography analyses. The *Aliivibrio Fischeri* bacterium was purchased from BioLight Multi Reagent for acute toxicity analysis. All solutions were prepared with double-deionized water from a Millipore Milli-Q system (18.2 mΩ cm, 25 °C).

2.2. Experimental procedure

Electrochemical oxidation experiments were performed using a single-compartment parallel flow electrochemical cell in batch operation mode [29]. BDD, purchased from NeoCoat (Switzerland), and different MMOs (Tianode, India) were used as anode material. SS plates were employed as cathode material. All electrodes were circular, with an electrode gap of 9 mm and an active area of 78 cm^2. The treatment of urban treated wastewater polluted with NPs was carried out under galvanostatic conditions by applying current densities within the range of 10 and 100 mA cm^{-2}.

Synthetic urban treated wastewater was prepared to simulate the physical–chemical composition of actual urban treated wastewater that typically comes from the secondary clarifier of an urban WWTP [30]. This complex effluent was contaminated with 20 mg L^{-1} polystyrene nanoplastics. Table 1 shows the composition of the synthetic urban treated wastewater used in this work. A volume of 1.5 L of polluted synthetic urban treated wastewater was introduced into the feed tank and continuously recirculated with a peristaltic pump, previously passing through the electrochemical cell. The temperature was maintained at 25 °C in the feed tank and at the outlet of the electrochemical cell with a thermostatized bath (JP Selecta, Spain). A detail of the experimental set-up is included in the supplementary material (Fig. S1).

2.3. Analytical techniques

Total Organic Carbon (TOC) was measured using a Shimadzu TOC-V CSH analyser. Ion chromatography (IC) was used to determine the concentration of inorganic ions using a Metrohm 930 Compact IC Flex coupled to a conductivity detector. A Metrosep A Supp 5 250/4.0 column was used to measure anions, and a Metrosep C6 250/4.0 column was used to analyse the cations. The mobile phase consisted of Na_2CO_3 (3.2 μM) and $NaHCO_3$ (1 μM) with a flow rate of 0.7 mL min^{-1} for determining anions and 1.7 mM HNO_3 and 1.7 mM oxalic acid solution for determining cations (flow rate: 1.0 mL min^{-1}). The injection volume of each sample was 20 μL. Total oxidants were quantified using the iodometric method reported by Kolthoff & Carr [31]. A 905 Titrando system (Methrom Hispania, Spain) with 0.005 M $Na_2S_2O_3$ as titration solution was employed. A pH/EC/TDS Meter HI991301 (Hanna) was used to measure pH and conductivity. All measurements were done in triplicate.

The morphological changes of NPs during the electrochemical treatment were analysed using a JEOL JEM 2100 HT transmission electron microscope (TEM). This high-resolution TEM operates at an accelerating voltage of 200 kV, which allows detailed images of

Table 1
Composition of synthetic urban treated wastewater.

Parameter	Value
Cl^- (mg L^{-1})	149.50
SO_4^{2-} (mg L^{-1})	300.00
NO_3^- (mg L^{-1})	5.00
PO_4^{3-} (mg L^{-1})	5.00
CH_3COO^- (mg L^{-1})	39.53
NH_4^+ (mg L^{-1})	2.00
Na^+ (mg L^{-1})	163.50
K^+ (mg L^{-1})	81.45
Mg^{2+} (mg L^{-1})	25.30
NPs (mg L^{-1})	20.00
TOC (mg L^{-1})	34.33 (15.87 without NPs)
COD (mg L^{-1})	94 (39 without NPs)
Turbidity (NTU)	24.00
pH	6.40
Conductivity (μS cm^{-1})	1450.00

nanoscale structures to be obtained. The resulting TEM micrographs were analysed to obtain quantitative information about particle size and shape characteristics. This analysis was conducted using the open-source software ImageJ, which provides tools for precise measurements and statistical analysis of the micrographs.

Acute toxicity towards the *Aliivibrio fischeri* (marine luminescent bacterium) was determined by a BioLight Toxy Analyzer (Microbiotest). Toxic effects were quantified over the changes in the light emission of the marine luminescent bacterium according to ISO 11348–3. Briefly, lyophilised bacteria were reconstituted by suspension in 1 mL of Bio-Light bio-recognition solution. Then, 10 μL of reconstituted bacterial suspension was added to 0.5 mL of BioLight diluent, and the light emission was recorded after 15 min (blank sample). Immediately after, treated samples were analysed, and toxic effects were monitored as a luminescence percentage decrease of the *Aliivibrio fischeri* bacterium at 15 min.

3. Results and discussion

The characterisation of NPs in wastewater is not straightforward and generally cannot be carried out directly. One of the strategies proposed in the literature for quantifying the concentration of NPs during applying AOPs is the measurement of TOC [13]. This parameter informs about the total mineralisation of the organic matter present in the effluents and, hence, it is an indicator that NPs have been removed. Fig. 1 shows the evolution of TOC during the treatment of synthetic urban wastewater polluted with 20 mg L^{-1} NPs by electrochemical oxidation with BDD anodes at different current densities.

As can be observed, the TOC concentration decreases with the operation time for all the current densities studied. The higher the current density, the higher the TOC removal. Specifically, TOC removal percentages of 52, 91 and 97 % are achieved when applying current densities of 10, 50, and 100 mA cm^{-2}, respectively. This reveals that it is possible to almost wholly degrade NPs in urban treated wastewater at higher current densities (> 50 mA cm^{-2}). The trend observed suggests that a complete mineralisation will be achieved at higher operation times. Nonetheless, it is important to note that TOC measured involves all the organic matter in the effluent: NPs and acetate. Hence, the mineralisation percentage achieved includes the degradation of both NPs and acetate. To shed light on the selective degradation of NPs by electrochemical oxidation with BDD anodes, the removal of NPs in synthetic urban treated wastewater without acetate was carried out (Fig. S2). Results show a decrease in the NPs concentration, reaching removal percentages of 12, 37 and 61 % in 180 min when working at 10, 50 and 100 mA cm^{-2}, respectively. This demonstrates the ability of the electrochemical oxidation with BDD anodes to degrade NPs in complex effluents.

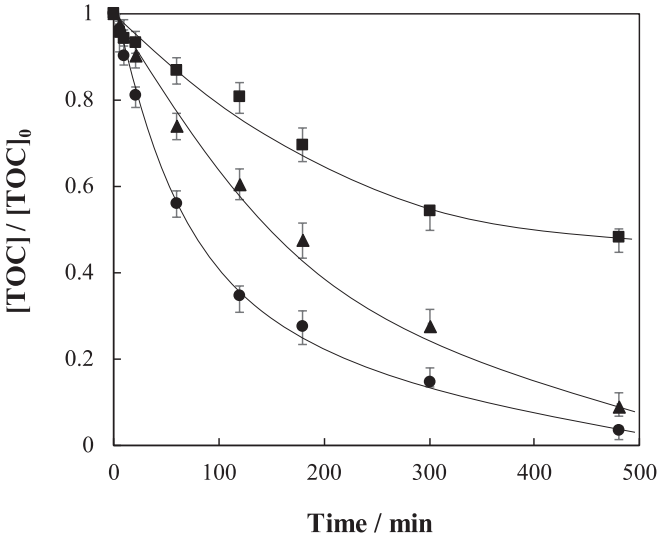

Fig. 1. Influence of the current density on TOC removal during the treatment of synthetic urban treated wastewater polluted with NPs. (■) 10 mA cm^{-2}; (▲) 50 mA cm^{-2}; (●) 100 mA cm^{-2}; $[NPs]_0$: 20 mg L^{-1}; $[TOC]_0$: 34.33 mg L^{-1}; anode: BDD; cathode: SS; T: 25 °C.

Experimental data were fitted to a first-order kinetics model using Equation (1), where C_0 is the initial TOC concentration in mg L^{-1}, C is the TOC concentration at the given time in mg L^{-1}, k is the kinetic constant in min^{-1}, and t is the operation time in min. The calculated kinetic constants are shown in Table 2.

$$\mathrm{Ln}\ (C_0/C) = k \cdot t \quad (1)$$

As expected, the highest kinetic constant is obtained when working at 100 mA cm^{-2} since the results plotted in Fig. 1 show a faster TOC decay. The differences observed between the calculated kinetic constants at current densities above 50 mA cm^{-2} and the lowest value (10 mA cm^{-2}) reveal that it is necessary to apply a minimum current density of 50 mA cm^{-2} to ensure a remarkable TOC decrease (> 90 %). However, the fact that the mineralisation process is faster does not indicate that it is more efficient from an electrochemical viewpoint. For this reason, the specific efficiency (η) of TOC removal was calculated according to Equation (2), where $[TOC]_0$ represents the initial concentration of TOC in the synthetic urban treated wastewater and $[TOC]_i$ denotes the concentration of TOC achieved at a specified applied electric charge (Q_i). Two different electric charges were selected (1 and 5 Ah L^{-1}), and the results are shown in Fig. 2. TOC evolution as a function of the applied electric charge at different current densities is plotted in Fig. S3.

$$\eta\ (\mathrm{mg\ TOC\ A^{-1}\ h^{-1}}) = \frac{[TOC]_0 - [TOC]_i}{Q_i} \quad (2)$$

Increasing the current density and the applied electric charge decreases the TOC removal efficiency. At low current densities (10 mA cm^{-2}), the values obtained cut down from 16.87 to 9.77 mg TOC $A^{-1}h^{-1}$, corresponding to 17.06 and 50.49 % mineralisation percentages, respectively. Current densities above 50 mA cm^{-2} show TOC removal efficiencies of around 9.35 mg TOC $A^{-1}h^{-1}$ at 1 Ah L^{-1}, decreasing to values close to 6.80 mg TOC $A^{-1}h^{-1}$ at 5 Ah L^{-1}. In this case, the mineralisation percentages achieved are around 10 and 36 % when passing 1 and 5 Ah L^{-1} at 50 and 100 mA cm^{-2}, respectively. These results confirm that TOC removal efficiency improves at low current densities because the mineralisation percentage for a specific applied electric charge increases at 10 mA cm^{-2}. This is an expected behaviour because the electrochemical oxidation of low concentrations of organics using BDD anodes is predominantly controlled by mass transport processes, where the higher the current density, the lower the efficiency [22]. The oxygen evolution or dimerisation can be favoured during the process at high current densities, competing with the mineralisation of NPs and decreasing the TOC removal efficiency [22,32].

NPs mineralisation can be achieved by directly oxidising the pollutants on the anode surface or by mediated oxidation by radicals and oxidants in situ electrochemically generated during the process [33]. Working at low current densities, mediated oxidation is not expected to be the primary oxidation mechanism, while the formation of oxidants is promoted working at high current densities [34]. Inorganic ions present in synthetic urban treated wastewater represent a potential source of oxidants in addition to hydroxyl radicals formed by water oxidation on

Table 2
TOC removal kinetic constants.

j (mA cm^{-2})	k (min^{-1})	S_R^2 ($mg^2\ L^{-2}$)	R^2
10	0.0016	0.00252	0.9643
50	0.0049	0.00744	0.9885
100	0.0068	0.01202	0.9904

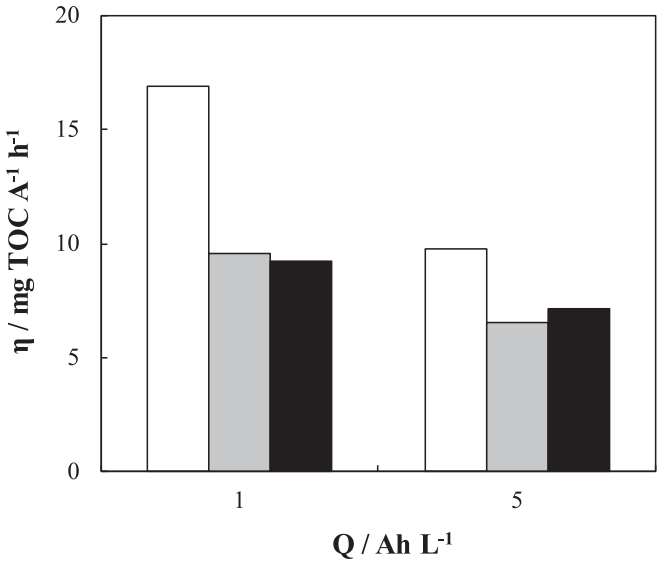

Fig. 2. Influence of current density on the specific TOC removal efficiency during the treatment of synthetic urban treated wastewater polluted with NPs. (□) 10 mA cm^{-2}; (▒) 50 mA cm^{-2}; (■) 100 mA cm^{-2}; $[NPs]_0$: 20 mg L^{-1}; $[TOC]_0$: 34.33 mg L^{-1}; anode: BDD; cathode: SS; T: 25 °C.

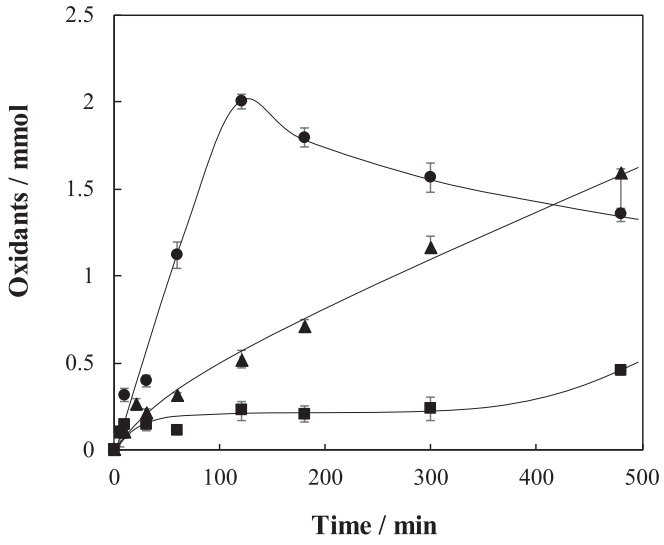

Fig. 3. Evolution of oxidants during the treatment of synthetic urban treated wastewater polluted with NPs. (■) 10 mA cm^{-2}; (▲) 50 mA cm^{-2}; (●) 100 mA cm^{-2}; $[NPs]_0$: 20 mg L^{-1}; $[TOC]_0$: 34.33 mg L^{-1}; anode: BDD; cathode: SS; T: 25 °C.

the anode surface (Equation (3). These oxidants can react with and degrade the organic matter in the effluent until its complete mineralisation. Specifically, anions such as chloride, sulphate, or phosphate can be electrochemically oxidised to hypochlorite, persulphate, and peroxydiphosphate, respectively, on BDD anodes (Equations (4)–(8) [22].

$$H_2O \rightarrow H^+ + HO\cdot + e^- \quad (3)$$

$$2\ Cl^- \rightarrow Cl_2 + 2\ e^- \quad (4)$$

$$Cl_2 + H_2O \rightarrow HClO + Cl^- + H^+ \quad (5)$$

$$HClO \leftrightarrows H^+ + ClO^- \quad (6)$$

$$2\ SO_4^{2-} \rightarrow S_2O_8^{2-} + 2\ e^- \quad (7)$$

$$2\ PO_4^{3-} \rightarrow P_2O_8^{4-} + 2\ e^- \quad (8)$$

Furthermore, anions can also react with the electrogenerated hydroxyl radicals to form other free radicals and oxidants in the effluent (Equations (9)–(14) [22].

$$Cl^- + HO\cdot \rightarrow Cl\cdot + OH^- \quad (9)$$

$$Cl\cdot + Cl\cdot \rightarrow Cl_2 \quad (10)$$

$$SO_4^{2-} + HO\cdot \rightarrow SO_4\cdot^- + OH^- \quad (11)$$

$$SO_4\cdot^- + SO_4\cdot^- \rightarrow S_2O_8^{2-} \quad (12)$$

$$PO_4^{3-} + HO\cdot \rightarrow PO_4\cdot^{2-} + OH^- \quad (13)$$

$$PO_4\cdot^{2-} + PO_4\cdot^{2-} \rightarrow P_2O_8^{4-} \quad (14)$$

The concentration of total oxidants was measured to confirm the presence of oxidant species during the electrochemical treatment of synthetic urban treated wastewater polluted with NPs using BDD anodes. Fig. 3 shows the evolution of these species with time at different current densities.

As can be observed, the oxidant concentration increases with the operation time for all the tests carried out, regardless of the current density applied. These results confirm the ability of BDD anodes to generate powerful oxidants in synthetic urban treated wastewater polluted with NPs. However, it is important to note that the oxidant concentration plotted in Fig. 3 reflects only the free oxidants that have not yet reacted at a given time rather than the total amount of these species that have been electrogenerated and have already reacted with the organic matter contained in the effluent. The higher the current density, the higher the maximum concentration of oxidants reached. Specifically, maximum oxidant amounts of 0.46, 1.59, and 2.00 mmol are reached for current densities of 10, 50, and 100 mA cm^{-2}, respectively. The trends observed in the oxidant concentration profiles indicate the influence of the current density on the generation of these species. At current densities of 10 and 50 mA cm^{-2}, the maximum concentration reached corresponds to the final concentration measured. In contrast, at a higher current density of 100 mA cm^{-2}, the concentration initially increases to the maximum value at about 120 min, followed by a slight decrease at the end of the experiment. This behaviour reveals that the oxidant generation and consumption rates start to be similar at the end of the process at high current densities, and it could be related to a possible recombination of these species.

From Fig. 3, it can be confirmed that oxidant species are generated during the electrochemical treatment of synthetic urban treated wastewater with BDD anodes, suggesting that the degradation of NPs is favoured by mediated oxidation. Electrogenerated hydroxyl radicals can attack C–H and C–C bonds of the polymeric structure by hydrogen abstraction and recombination reactions, promoting the formation of other organics such as styrene, acetophenone or benzaldehyde. Furthermore, these radicals can be added to the aromatic rings and generate peroxyl radicals, which are converted to alcohols, ketones, and carboxylic acids during the electrochemical treatment. These products are continuously degraded to low molecular weight organics until their complete mineralisation [35]. Likewise, electrogenerated sulphate radicals can extract a hydrogen atom from the lateral chains or the main polymeric structure, promoting the generation of radicals. In addition, sulphate radicals can react with benzenic rings and form compounds with sulphate or sulphonate groups. Next, the reaction with oxygen and sulphate radicals promotes the formation of oxidized species, resulting in alcohols, ketones, and carboxylic acids from the oxidation of the main structure of polystyrene and sulfonated or sulphated derivatives by the addition of sulphate groups to the main and lateral chains. These compounds are continuously oxidised until their complete mineralisation. To assess the contributions of mediated oxidation by hydroxyl and sulphate radicals, the degradation of 20 mg L^{-1} NPs was carried out in an inert media (0,3 g L^{-1} $HClO_4$) with a conductivity matching that of synthetic urban treated wastewater at a current density of 100 mA cm^{-2}

(Fig. S4). Under these conditions, NPs removal can only occur directly at the anode surface or via mediation by hydroxyl radicals due to the high applied current density [36]. The results indicated that NPs degradation was approximately 30 % lower in the inert media, confirming that hydroxyl radicals are primarily responsible for NPs removal in synthetic urban treated wastewater (with 70 % NPs removal observed in perchloric acid). In contrast, sulphate radicals in the urban treated wastewater further enhanced NPs degradation, achieving up to 97 % reduction in NPs concentration.

The attack of electrogenerated oxidants and radicals on NPs can change their morphology, and hence, a transmission electronic microscopy (TEM) analysis was carried out. Fig. 4 shows TEM images of different samples obtained during the degradation of NPs in synthetic urban treated wastewater by electrochemical oxidation with BDD anodes at 100 mA cm^{-2}. This experiment was selected because the mineralisation percentage was nearly 100 % (Fig. 1).

At the beginning of the process, NPs are perfect polystyrene spheres with a diameter of 150 nm. Applying a specific current density induces the breakdown of the polymer chains by the attack of the oxidants and free radicals electrogenerated, promoting the agglomeration of particles (Fig. 4b). In addition, NPs are degraded from the surface to the core, decreasing their particle size to 110 nm but retaining their morphology (Fig. 4c). The size and volume of NPs are significantly reduced at the end of the treatment (Fig. 4d), reaching a particle size of 68 nm. On the other hand, TEM images show NPs with two areas (different contrasts) that are related to the synthesis process of the particles (emulsion polymerization, precipitation polymerization, physical fragmentation, etc.). Other AOPs have also observed this behaviour during the degradation of polystyrene NPs in ultrapure water [27].

The concentration of NPs in wastewater can vary significantly, depending on their source and nature. The removal of high concentrations of NPs from synthetic urban treated wastewater by electrochemical oxidation with BDD anodes was also studied to address this issue. A current density of 100 mA cm^{-2} was selected based on its previously demonstrated efficiency in achieving optimal mineralisation rates (Fig. 1). The initial concentration of NPs increased to 100 mg L^{-1}. The results of the electrochemical oxidation process are depicted in Fig. 5.

As can be observed, TOC decreases with the operation time during the electrochemical oxidation with BDD anodes at 100 mA cm^{-2}, regardless of the initial NPs concentration. However, the final mineralisation percentage achieved is influenced by the initial pollutant concentration, reaching 97 and 88 % values at initial NPs concentrations of 20 and 100 mg L^{-1}, respectively. This leads to a decrease in the kinetic constant from 0.0068 to 0.0044 min^{-1} when the initial concentration increases from 20 to 100 mg L^{-1} (inset of Fig. 5).

Increasing the initial NPs concentration (100 mg L^{-1}) may result in forming many intermediate species competing for electrogenerated oxidants or reaction sites (direct oxidation), decreasing the reaction rate and the process efficiency. Therefore, a higher concentration of oxidants in the effluent will be required to ensure a mineralisation rate similar to that obtained when working with 20 mg L^{-1} NPs. This could be achieved by working at higher current densities (> 100 mA cm^{-2}), although it would considerably increase the energy requirements of the technology.

A five-fold increase of the initial NPs concentration results in a mineralisation percentage decrease of less than 10 % under the same operating conditions. These findings demonstrate the robustness of electrochemical oxidation with BDD anodes to remove NPs from complex effluents.

Once electrochemical oxidation with BDD anodes has been proven efficient for removing NPs from synthetic urban treated wastewater, the influence of the anode material was evaluated. For this purpose, different Mixed Metal Oxide (MMO) anodes were used to treat effluents polluted with 20 mg L^{-1} NPs: Pt/Ti, RuO_2/Ti and IrO_2/Ti. Fig. 6 shows the evolution of TOC during the treatment of synthetic urban treated wastewater polluted with 20 mg L^{-1} NPs by electrochemical oxidation at 100 mA cm^{-2} with different anodes.

When working with MMO anodes at a current density of 100 mA cm^{-2}, a negligible TOC mineralisation percentage is observed compared to the results obtained with BDD anodes. Specifically, 0.16, 0.23 and 6.49 % TOC removal percentages are achieved using IrO_2/Ti, RuO_2/Ti and Pt/Ti, respectively, whereas BDD anodes results in a mineralisation percentage of 97 %. This behaviour is clearly due to the different electrocatalytic properties of each anodic material, which are related to the interactions between the free radicals electrogenerated (mainly hydroxyl radicals) and the electrode material. MMO anodes are classified as active electrodes because the radicals generated during the electrochemical oxidation are chemisorbed on their surface (Equation (15) [25,37]. This promotes the incorporation of radicals into the anode

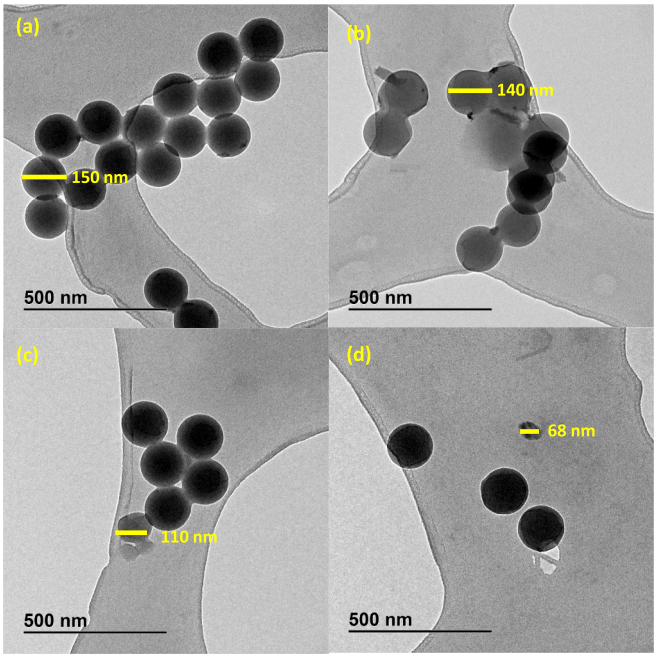

Fig. 4. TEM analysis for the electrochemical treatment of synthetic urban treated wastewater polluted with NPs. (a) 0 min; (b) 60 min; (c) 180 min; (d) 480 min; j: 100 mA cm^{-2}; $[NPs]_0$: 20 mg L^{-1}; $[TOC]_0$: 34.33 mg L^{-1}; anode: BDD; cathode: SS; T: 25 °C.

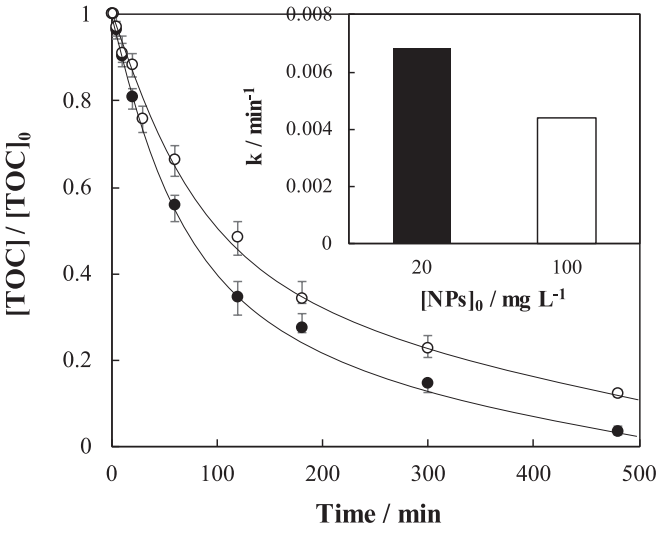

Fig. 5. Influence of the initial NPs concentration on TOC removal during the treatment of synthetic urban treated wastewater polluted with NPs. (●) 20 mg L^{-1}; (○) 100 mg L^{-1}; j: 100 mA cm^{-2}; anode: BDD; cathode: SS; T: 25 °C.

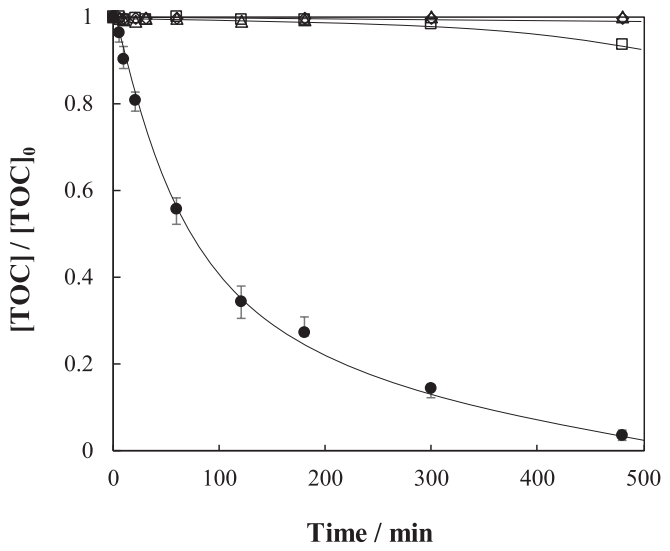

Fig. 6. Influence of the anode material on TOC removal during the treatment of synthetic urban treated wastewater polluted with NPs. (●) BDD; (□) Pt/Ir; (Δ) RuO_2/Ti; (○) IrO_2/Ti; $[NPs]_0$: 20 mg L^{-1}; $[TOC]_0$: 34.33 mg L^{-1}; j: 100 mA cm^{-2}; cathode: SS; T: 25 °C.

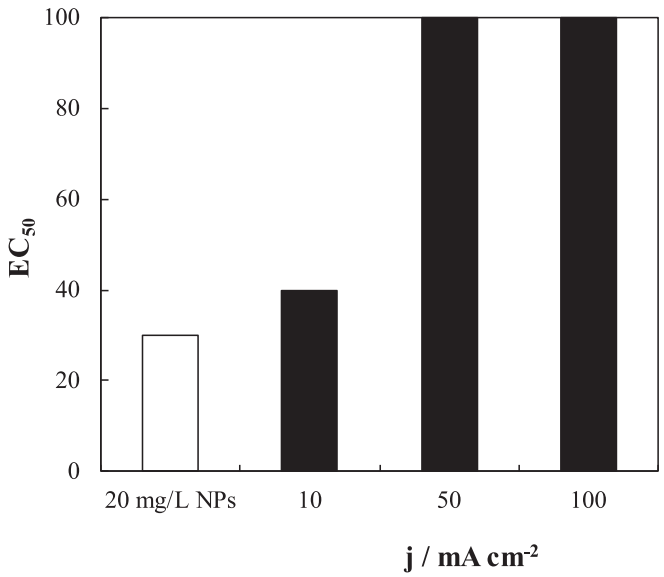

Fig. 7. EC_{50} values after the electrochemical oxidation of synthetic urban treated wastewater polluted with NPs. $[NPs]_0$: 20 mg L^{-1}; $[TOC]_0$: 34.33 mg L^{-1}; anode: BDD; cathode: SS; T: 25 °C.

material, forming surface-bound oxidised species instead of allowing the radicals to diffuse freely into the solution. On the contrary, BDD anodes are known as non-active electrodes in which radicals are physisorbed. In this case, radicals are released into the effluent, enabling the complete degradation of organics to CO_2 and H_2O (Equations (16)–(17). Hence, there is a strong interaction between radicals and MMO anodes and a weak interaction with BDD anodes. This explains the differences observed with each anodic material during the electrochemical oxidation and supports that the removal of NPs from synthetic urban treated wastewater is mainly due to a mediated oxidation mechanism.

$$MMO + H_2O \rightarrow MMO(HO\cdot) + H^+ + e^- \quad (15)$$

$$BDD + H_2O \rightarrow BDD(HO\cdot) + H+ + e^- \quad (16)$$

$$BDD(HO\cdot) + \text{organics} \rightarrow BDD + CO_2 + H_2O \quad (17)$$

Furthermore, BDD anodes can electrochemically generate powerful oxidants such as peroxocompounds (Equations (7)–(8), (11)–(14)), which significantly contribute to the degradation of NPs, whereas MMO anodes promote the formation of large amounts of free chlorine (Equations (4)–(6) [38]. This different nature of the oxidants electrogenerated with one electrode or the other also influences the degradation of organics [39].

Once electrochemical oxidation with BDD anodes has been proven efficient for the degradation of NPs from urban treated wastewater, the luminescence inhibition using the *Aliivibrio fischeri* bacterium evaluated the acute toxicity of treated effluents. Toxicity was measured with the EC_{50} value, representing the sample concentration required to produce a 50 % bacterial inhibition. Fig. 7 shows the EC_{50} values obtained for the initial synthetic urban treated wastewater polluted with 20 mg L^{-1} NPs and the final samples of the experiments at different current densities.

The toxicity of synthetic urban treated wastewater without NPs was first measured to ensure that the physical–chemical composition of the effluent used did not contribute to acute toxicity, resulting in an EC_{50} of 100. The untreated effluent containing 20 mg L^{-1} NPs shows an EC_{50} value of 29.93 %, indicating the acute toxicity of these pollutants. This is an expected result because NPs are known to cause physical interference and oxidative stress in aquatic organisms. In particular, they can disrupt cellular functions and even induce inflammation or toxicity through interactions with cell membranes due to their small size [40].

After the electrochemical treatment at a current density of 10 mA cm^{-2}, the EC_{50} increases to 39.97 %, showing a slight reduction in acute toxicity. This suggests that the NPs degradation produces less toxic fragments. Under these operating conditions, a TOC removal of 50 % was achieved (Fig. 1), corresponding to a partial NPs removal and, consequently, to a slight reduction of their toxicity, as shown in Fig. 7. Increasing the current density to 50 and 100 mA cm^{-2} leads to a complete reduction of the acute toxicity in treated effluents, with EC_{50} values of 100 %. This demonstrates that mineralisation percentages exceeding 90 % ensure a total decrease of acute toxicity. Furthermore, these results suggest that the remaining TOC in the synthetic urban treated wastewater after the electrochemical oxidation at high current densities consists primarily of harmless intermediate compounds formed during the degradation of NPs since the acute toxicity is wholly removed from the treated effluents.

The significant reduction in toxicity is corroborated by the recovery of the *Aliivibrio fischeri* bacterium luminescence, indicating that bacterial cells are less affected by the treated effluent. This increase in bioluminescence confirms that the proposed electrochemical treatment effectively mitigates the acute toxic effects of NPs.

Finally, the energy consumption per unit volume (W) was estimated following Equation (18), where Q is the applied electric charge in kAh m^{-3} and V is the applied voltage in volts (V).

$$W\ (kWh\ m^{-3}) = Q \cdot V \quad (18)$$

The energy consumption has been calculated for the TOC reduction of 50 %, and the final TOC reduction registered at the end of the experiments at different current densities. Results are summarised in Table 3.

As expected, the energy consumption increases with the current density since the applied voltage increases with this parameter. At low current densities (10 mA cm^{-2}), achieving 50 % TOC removal requires minimal energy consumption (37.16 kWh m^{-3}), as the applied electric

Table 3
Energy consumption.

j (mA cm^{-2})	10		50		100	
TOC removed (%)	50	52*	50	91*	50	97*
Q (kAh m^{-3})	4.82	5.54	8.63	26.60	7.83	55.44
Time (h)	7	8	2.80	8	1.30	8
W (kWh m^{-3})	37.16	42.69	151.47	429.79	197.49	1317.78

* TOC percentage removed at the end of the experiment.

charge needed is almost half compared to the values required at higher current densities. However, this operation requires 7 h to reach 50 % TOC removal, and even extending the treatment to 8 h only slightly increases removal to 52 %, with an energy consumption of 42.69 kWh m^{-3}. In contrast, working at 50 mA cm^{-2} achieves 50 % TOC removal in only 2.80 h with an energy consumption of 151.47 kWh m^{-3}, and extending the operation to 8 h raises the removal efficiency to 91 %, consuming 429.79 kWh m^{-3}. At 100 mA cm^{-2}, 50 % TOC removal is achieved in just 1.30 h but at a higher energy consumption of 197.49 kWh m^{-3} and extending to 8 h achieves the highest removal efficiency (97 %) but with an exceptionally high energy consumption of 1317.78 kWh m^{-3}.

As mentioned above, the final energy consumption at 10 mA cm^{-2} for extended operation (8 h) does not differ significantly from that required to remove 50 % of TOC due to the limited increase in removal efficiency (52 %). However, at higher current densities (50 and 100 mA cm ^{2}), removal percentages above 90 % can be achieved within 8 h, albeit with vastly different energy consumptions. Operating at 50 mA cm^{-2} offers a significant advantage, achieving 91 % removal with an energy consumption three times lower than 100 mA cm^{-2} when reaching a TOC removal of 97 %. This is because the electric charge required to surpass 90 % TOC removal at 50 mA cm^{-2} is approximately half that required at 100 mA cm^{-2}, with only a slight reduction in removal efficiency (6 %).

The energy consumption observed in this study indicates that there is potential for improving energy efficiency in the process. However, in the study conducted by Kiendrebeogo et al. [26], where they investigated the removal of 10 mg L^{-1} of polystyrene nanoplastics in a sulphate medium at a current density of 36 mA cm^{-2}, the reported energy consumption was 363.8 kWh m^{-3}, achieving a mineralization rate of 56.2 %. This value is significantly higher than the energy consumption obtained in the present work (151.47 kWh m^{-3}) despite operating at a higher current density (50 mA cm^{-2}) and achieving a comparable mineralization rate of 50 %.

From an energy-efficiency viewpoint, 50 mA cm^{-2} is the most favourable operating condition. While 10 mA cm^{-2} minimizes energy consumption, it requires prolonged operation and yields only modest TOC removal rates. On the other hand, 100 mA cm^{-2} achieves the highest TOC removal percentage but at the cost of excessive energy consumption. Therefore, a current density of 50 mA cm^{-2} provides an optimal balance between high TOC removal efficiency and reasonable energy consumption, making it the preferred choice for practical applications.

4. Conclusions

From this work, the following conclusions can be drawn:

- Electrochemical oxidation with BDD anodes can degrade polystyrene NPs in synthetic urban treated wastewater, applying current densities above 50 mA cm^{-2}. Using low current densities (10 mA cm^{-2}) leads to mineralisation percentages around 50 %, whereas increasing to 50 and 100 mA cm^{-2}, the values obtained are 91 and 97 %, respectively. The generation of powerful oxidants during the electrochemical oxidation significantly influences the mineralisation of the organic matter.
- Increasing current density enhances mineralisation rates but reduces the electrochemical efficiency due to side reactions like oxygen evolution during the process with BDD anodes. TEM analysis further confirms the gradual degradation of NPs, with particle sizes reduced from 150 nm to 68 nm during treatment. On the other hand, the robustness of the technology is demonstrated through its ability to handle varying initial NP concentrations, with minor efficiency reductions at higher pollutant loads. These findings validate electrochemical oxidation with BDD anodes as a sustainable, efficient, and adaptable solution for treating wastewater polluted with NPs.
- The use of MMO anodes is unsuitable for degrading NPs by electrochemical oxidation. TOC removal percentages lower than 6.50 % are obtained using IrO_2/Ti, RuO_2/Ti and Pt/Ti anodes. This confirms that the degradation of polystyrene NPs by electrochemical oxidation is mainly favoured by a mediated oxidation mechanism involving the attack of electrogenerated oxidants.
- Acute toxicity of treated effluents at current densities above 50 mA cm^{-2} was completely reduced ($EC_{50} = 100$) due to the almost complete mineralisation of the organic matter (> 90 %). This suggests that the by-products formed during the degradation of NPs by electrochemical oxidation with BDD anodes are non-toxic. It also highlights the environmental safety of the treated effluents.

Overall, this work opens new pathways for applying electrochemical technologies to mitigate nanoplastics pollution, protect aquatic environments, and support global efforts to address emerging contaminants.

Declaration of competing interest

The authors declare that they have no known competing financial interests or personal relationships that could have appeared to influence the work reported in this paper.

Acknowledgements

This research is part of the project TED2021-131380A-C22 (REGENEDAR), funded by MCIN/AEI/10.13039/501100011033 and the European Union NextGenerationEU/PRTR, and the network RED2022-134552-T (E3TECH+) funded by MICIU/AEI/10.13039/501100011. Grant CNS2023-144029 funded by MICIU/AEI/10.13039/501100011033 and by European Union NextGenerationEU/PRTR, and project TEC-2024/ECO-69 (CARESOIL-CM) funded by the Community of Madrid are also acknowledged.

Appendix A. Supplementary data

Supplementary data to this article can be found online at https://doi.org/10.1016/j.seppur.2025.132139.

Data availability

Data will be made available on request.

References

[1] B.C. Park, A. Brown, F. Laubinger, P. Börkey, Monitoring Trade in Plastic Waste and Scrap (2024), https://doi.org/10.1787/013bcfdd-en.
[2] D.K.A. Barnes, F. Galgani, R.C. Thompson, M. Barlaz, Accumulation and fragmentation of plastic debris in global environments, Philos. Trans. R. Soc., B 364 (2009) 1985–1998, https://doi.org/10.1098/rstb.2008.0205.
[3] . Europe, Plastics—The Fast Facts 2023, (2023).
[4] A.L. Andrady, Microplastics in the marine environment, Mar. Pollut. Bull. 62 (2011) 1596–1605, https://doi.org/10.1016/j.marpolbul.2011.05.030.
[5] S. Gesamp, fate and effects of microplastics in the marine environment: part 2 of a global assessment.(IMO, FAO/UNESCO-IOC/UNIDO/WMO/IAEA/UN/UNEP/UNDP), Rep. Stud. GESAMP, (2016) 96.
[6] Y. Zhang, Y. Li, F. Su, L. Peng, D. Liu, The life cycle of micro-nano plastics in domestic sewage, Sci. Total Environ. 802 (2022) 149658, https://doi.org/10.1016/j.scitotenv.2021.149658.
[7] J. Gigault, B. Pedrono, B. Maxit, A. ter halle, Marine plastic litter: The unanalyzed nano-fraction, Environ. Sci.: Nano 3 (2016), https://doi.org/10.1039/C6EN00008H.
[8] M.A. Browne, P. Crump, S.J. Niven, E. Teuten, A. Tonkin, T. Galloway, R. Thompson, Accumulation of microplastic on shorelines woldwide: sources and sinks, Environ. Sci. Technol. 45 (2011) 9175–9179, https://doi.org/10.1021/es201811s.
[9] J. Sun, X. Dai, Q. Wang, M.C.M. van Loosdrecht, B.-J. Ni, Microplastics in wastewater treatment plants: Detection, occurrence and removal, Water Res. 152 (2019) 21–37, https://doi.org/10.1016/j.watres.2018.12.050.
[10] Z. Steinmetz, C. Wollmann, M. Schaefer, C. Buchmann, J. David, J. Tröger, K. Muñoz, O. Frör, G.E. Schaumann, Plastic mulching in agriculture. Trading short-

term agronomic benefits for long-term soil degradation? Sci. Total Environ. 550 (2016) 690–705, https://doi.org/10.1016/j.scitotenv.2016.01.153.
[11] S. Singh, T.S.S. Kumar Naik, A.G. Anil, J. Dhiman, V. Kumar, D.S. Dhanjal, L. Aguilar-Marcelino, J. Singh, P.C. Ramamurthy, Micro (nano) plastics in wastewater: A critical review on toxicity risk assessment, behaviour, environmental impact and challenges, Chemosphere 290 (2022) 133169, https://doi.org/10.1016/j.chemosphere.2021.133169.
[12] J. Gigault, A.T. Halle, M. Baudrimont, P.-Y. Pascal, F. Gauffre, T.-L. Phi, H. El Hadri, B. Grassl, S. Reynaud, Current opinion: What is a nanoplastic? Environ. Pollut. 235 (2018) 1030–1034, https://doi.org/10.1016/j.envpol.2018.01.024.
[13] C. di Luca, J. Garcia, M. Munoz, M. Hernando-Pérez, Z.M. de Pedro, J.A. Casas, Strategies for the quantification and characterization of nanoplastics in AOPs research, Chem. Eng. J., 493 (2024), https://doi.org/10.1016/j.cej.2024.152490.
[14] C. di Luca, J. Garcia, M. Munoz, L. Fasce, Z.M. de Pedro, J.A. Casas, Modeling polystyrene nanoplastics degradation in water via photo-Fenton treatment: A shrinking-particle approach, Appl Catal B 362 (2025), https://doi.org/10.1016/j.apcatb.2024.124751.
[15] J.R. Jambeck, R. Geyer, C. Wilcox, T.R. Siegler, M. Perryman, A. Andrady, R. Narayan, K.L. Law, Plastic waste inputs from land into the ocean, Science 347 (2015) 768–771, https://doi.org/10.1126/science.1260352.
[16] J. Li, H. Liu, J. Paul Chen, Microplastics in freshwater systems: A review on occurrence, environmental effects, and methods for microplastics detection, Water Res 137 (2018) 362–374, https://doi.org/10.1016/j.watres.2017.12.056.
[17] E.E. Burns, A.B.A. Boxall, Microplastics in the aquatic environment: Evidence for or against adverse impacts and major knowledge gaps, Environ Toxicol Chem 37 (2018) 2776–2796, https://doi.org/10.1002/etc.4268.
[18] C. Bretas Alvim, J.A. Mendoza-Roca, A. Bes-Piá, Wastewater treatment plant as microplastics release source – Quantification and identification techniques, J. Environ. Manage. 255 (2020) 109739, https://doi.org/10.1016/j.jenvman.2019.109739.
[19] Z. Xu, X. Bai, Microplastic Degradation in Sewage Sludge by Hydrothermal Carbonization: Efficiency and Mechanisms, Chemosphere 297 (2022) 134203, https://doi.org/10.1016/j.chemosphere.2022.134203.
[20] R.M. Blair, S. Waldron, C. Gauchotte-Lindsay, Average daily flow of microplastics through a tertiary wastewater treatment plant over a ten-month period, Water Res 163 (2019) 114909, https://doi.org/10.1016/j.watres.2019.114909.
[21] D. Angmo, J. Singh, S.A. Bhat, B. Thakur, A.P. Vig, Micro-Nano-Plastics in Sewage Sludge: Sources, Occurrence, and Potential Environmental Risks, in: S.A. Bhat, V. Kumar, F. Li, S. Kumar (Eds.), Management of Micro and Nano-Plastics in Soil and Biosolids: Fate, Occurrence, Monitoring, and Remedies, Springer Nature Switzerland, Cham, 2024, pp. 343–363.
[22] M. Herraiz-Carboné, A. Santos, A. Hayat, C.M. Domínguez, S. Cotillas, Remediation of groundwater polluted with lindane production wastes by conductive-diamond electrochemical oxidation, Sci. Total Environ. 926 (2024) 171848, https://doi.org/10.1016/j.scitotenv.2024.171848.
[23] D.M.D. Araújo, S. Cotillas, C. Sáez, P. Cañizares, C.A. Martínez-Huitle, M. A. Rodrigo, Activation by light irradiation of oxidants electrochemically generated during Rhodamine B elimination, J. Electroanal. Chem., 757 (2015) 144–149, https://doi.org/10.1016/j.jelechem.2015.09.025.
[24] S. Cotillas, M.J.M. de Vidales, J. Llanos, C. Sáez, P. Cañizares, M.A. Rodrigo, Electrolytic and electro-irradiated processes with diamond anodes for the oxidation of persistent pollutants and disinfection of urban treated wastewater, J. Hazard. Mater., 319 (2016) 93–101, https://doi.org/10.1016/j.jhazmat.2016.01.050.
[25] C.A. Martínez-Huitle, M.A. Rodrigo, I. Sirés, O. Scialdone, A critical review on latest innovations and future challenges of electrochemical technology for the abatement of organics in water, Appl Catal B 328 (2023) 122430, https://doi.org/10.1016/j.apcatb.2023.122430.
[26] M. Kiendrebeogo, M.R. Karimi Estahbanati, Y. Ouarda, P. Drogui, R.D. Tyagi, Electrochemical degradation of nanoplastics in water: Analysis of the role of reactive oxygen species, Sci. Total Environ. 808 (2022) 151897, https://doi.org/10.1016/j.scitotenv.2021.151897.
[27] C. di Luca, J. Garcia, D. Ortiz, M. Munoz, J. Carbajo, Z.M. de Pedro, J.A. Casas, Mineralization of polystyrene nanoplastics in water by photo-Fenton oxidation, J. Environ. Chem. Eng. 11 (2023) 110755, https://doi.org/10.1016/j.jece.2023.110755.
[28] I. Nabi, A.-U.-R. Bacha, K. Li, H. Cheng, T. Wang, Y. Liu, S. Ajmal, Y. Yang, Y. Feng, L. Zhang, Complete Photocatalytic Mineralization of Microplastic on TiO2 Nanoparticle Film, iScience, 23 (2020) 101326 Doi: 10.1016/j.isci.2020.101326.
[29] P. Cañizares, M. Díaz, J.A. Domínguez, J. García-Gómez, M.A. Rodrigo, Electrochemical Oxidation of Aqueous Phenol Wastes on Synthetic Diamond Thin-Film Electrodes, Ind. Eng. Chem. Res. 41 (2002) 4187–4194, https://doi.org/10.1021/ie0105526.
[30] A. Cano, C. Barrera, S. Cotillas, J. Llanos, P. Cañizares, M.A. Rodrigo, Use of DiaCell modules for the electro-disinfection of secondary-treated wastewater with diamond anodes, Chem. Eng. J. 306 (2016) 433–440, https://doi.org/10.1016/j.cej.2016.07.090.
[31] I.M. Kolthoff, E.M. Carr, Volumetric Determination of Persulfate in Presence of Organic Substances, Anal. Chem. 25 (1953) 298–301, https://doi.org/10.1021/ac60074a024.
[32] F.C. Moreira, R.A.R. Boaventura, E. Brillas, V.J.P. Vilar, Electrochemical advanced oxidation processes: A review on their application to synthetic and real wastewaters, Appl Catal B 202 (2017) 217–261, https://doi.org/10.1016/j.apcatb.2016.08.037.
[33] M. Panizza, G. Cerisola, Direct And Mediated Anodic Oxidation of Organic Pollutants, Chem. Rev. 109 (2009) 6541–6569, https://doi.org/10.1021/cr9001319.
[34] S. Cotillas, D. Clematis, P. Cañizares, M.P. Carpanese, M.A. Rodrigo, M. Panizza, Degradation of dye Procion Red MX-5B by electrolytic and electro-irradiated technologies using diamond electrodes, Chemosphere 199 (2018) 445–452, https://doi.org/10.1016/j.chemosphere.2018.02.001.
[35] Y. Yang, J. Chen, Z. Chen, Z. Yu, J. Xue, T. Luan, S. Chen, S. Zhou, Mechanisms of polystyrene microplastic degradation by the microbially driven Fenton reaction, Water Res. 223 (2022) 118979, https://doi.org/10.1016/j.watres.2022.118979.
[36] M. Herraiz-Carboné, S. Cotillas, E. Lacasa, Á. Moratalla, P. Cañizares, M. A. Rodrigo, C. Sáez, Improving the biodegradability of hospital urines polluted with chloramphenicol by the application of electrochemical oxidation, Sci. Total Environ. 725 (2020), https://doi.org/10.1016/j.scitotenv.2020.138430.
[37] K. Klyukin, A. Zagalskaya, V. Alexandrov, Role of Dissolution Intermediates in Promoting Oxygen Evolution Reaction at RuO2(110) Surface, J. Phys. Chem. C 123 (2019) 22151–22157, https://doi.org/10.1021/acs.jpcc.9b03418.
[38] M. Herraiz-Carboné, A. Santos, A. Checa-Fernández, C.M. Domínguez, S. Cotillas, Removal of organochlorine pollutants from DNAPL-saturated groundwater using electrolysis with MMO anodes, Chem. Eng. J., 486 (2024), https://doi.org/10.1016/j.cej.2024.150238.
[39] S. Cotillas, E. Lacasa, M. Herraiz, C. Sáez, P. Cañizares, M.A. Rodrigo, The Role of the Anode Material in Selective Penicillin G Oxidation in Urine, ChemElectroChem 6 (2019) 1376–1384, https://doi.org/10.1002/celc.201801747.
[40] Y. Ma, A. Huang, S. Cao, F. Sun, L. Wang, H. Guo, R. Ji, Effects of nanoplastics and microplastics on toxicity, bioaccumulation, and environmental fate of phenanthrene in fresh water, Environ. Pollut. 219 (2016) 166–173, https://doi.org/10.1016/j.envpol.2016.10.061.